Inorg. Chem. **2009**, *48*, 2571−2582

Catalytic Activity of Biscobalt Porphyrin-Corrole Dyads Toward the Reduction of Dioxygen

Karl M. Kadish,*,† Laurent Frémond,† Jing Shen,† Ping Chen,† Kei Ohkubo,‡ Shunichi Fukuzumi,*,‡ Maya El Ojaimi,§ Claude P. Gros,§ Jean-Michel Barbe,§ and Roger Guilard*,§

Department of Chemistry, University of Houston, Houston, Texas 77204-5003, Université de Bourgogne, ICMUB (UMR 5260), 9, Avenue Alain Savary, BP 47870, 21078 Dijon Cedex, France, Department of Material and Life Science, Graduate School of Engineering, Osaka University, SORST, Japan Science and Technology Agency (JST), Suita, Osaka 565-0871, Japan

Received October 31, 2008

A series of biscobalt cofacial porphyrin-corrole dyads bearing mesityl substituents at the *meso* positions of the corrole ring were investigated as to their electrochemistry, spectroelectrochemistry, and CO binding properties in nonaqueous media and then applied to the surface of a graphite electrode and tested as electrocatalysts for the reduction of dioxygen to water or hydrogen peroxide in air-saturated aqueous solutions containing 1 M $HClO_4$. The catalytic reduction of O_2 with the same dyads was also investigated in the homogeneous phase using 1,1′-dimethylferrocene as a reductant in PhCN containing $HClO_4$. The examined compounds are represented as $(PMes_2CY)Co_2$, where P = a porphyrin dianion, Mes_2C = a corrole trianion with two mesityl groups in *trans meso*-positions of the macrocycle, and Y is one of three bridging groups separating the two metallomacrocycles in a face-to-face arrangement, either with 9,9-dimethylxanthene, dibenzofuran, or diphenylether as linkers. Cyclic voltammetry and rotating disk electrode voltammetry revealed that the examined compounds are all catalytically active toward the electroreduction of dioxygen in acid media giving H_2O_2 or H_2O depending upon the type of linkage (Y) and the initial site of electron transfer which, in nonaqueous media, could be switched between the corrole and the porphyrin metal center by variations of substituents on the corrole macrocycle or the gas above the solution. The homogeneous reduction of dioxygen *via* a two- or four-electron transfer process was also investigated using 1,1′-dimethylferrocene as reductant in PhCN containing $HClO_4$.

Introduction

Extensive efforts have been devoted to developing innovative materials as catalysts for the four-electron electrochemical reduction of O_2 in energy conversion technologies such as fuel cells. A replacement of platinum metal which is now used as the catalyst in fuel cells is necessary because of its high cost and limited availability which has hindered commercialization.[1−7] In nature, cytochrome *c* oxidase and related heme/copper terminal oxidases act as the fuel cells of aerobic organisms, catalyzing the selective and complete four-proton, four-electron conversion of oxygen to water without releasing partially reduced peroxide (or superoxide) intermediates.[8−14] In this context, cofacial bimetallic por-

* To whom correspondence should be addressed. E-mail: kkadish@uh.edu (K.M.K.), fukuzumi@chem.eng.osaka-u.ac.jp (S.F.), roger.guilard@u-bourgogne.fr (R.G.).
† University of Houston.
‡ Osaka University.
§ Université de Bourgogne.

(1) Steele, B. C. H.; Heinzel, A. *Nature* **2001**, *414*, 345–352.
(2) Steele, B. C. H. *J. Mater. Sci.* **2001**, *36*, 1053–1068.
(3) Stamenkovic, V. R.; Fowler, B.; Mun, B. S.; Wang, G.; Ross, P. N.; Lucas, C. A.; Markovic, N. M. *Science* **2007**, *315*, 493–497.
(4) Zhang, J.; Sasaki, K.; Sutter, E.; Adzic, R. R. *Science* **2007**, *315*, 220–222.
(5) Yu, P.; Yan, J.; Zhao, H.; Su, L.; Zhang, J.; Mao, L. *J. Phys. Chem. C* **2008**, *112*, 2177–2182.
(6) Wang, C.; Daimon, H.; Lee, Y.; Kim, J.; Sun, S. *J. Am. Chem. Soc.* **2007**, *129*, 6974–6975.
(7) Ye, H.; Crooks, R. M. *J. Am. Chem. Soc.* **2007**, *129*, 3627–3633.
(8) Ferguson-Miller, S.; Babcock, G. T. *Chem. Rev.* **1996**, *96*, 2889–2907.
(9) Wikström, M. *Biochim. Biophys. Acta* **2000**, *1458*, 188–198.
(10) Zaslavsky, D.; Gennis, R. B. *Biochim. Biophys. Acta* **2000**, *1458*, 164–179.
(11) Pereira, M. M.; Santana, M.; Teixeira, M. *Biochim. Biophys. Acta* **2001**, *1505*, 185–208.
(12) Ostermeier, C.; Harrenga, A.; Ermler, U.; Michel, H. *Proc. Natl. Acad. Sci. U.S.A.* **1997**, *94*, 10547–10553.
(13) Yoshikawa, S.; Shinzawa-Itoh, K.; Tsukihara, T. *J. Inorg. Biochem.* **2000**, *82*, 1–7.

10.1021/ic802092n CCC: $40.75
Published on Web 02/12/2009

Chart 1. Structures of Investigated Biscobalt Porphyrin-Corrole Dyads

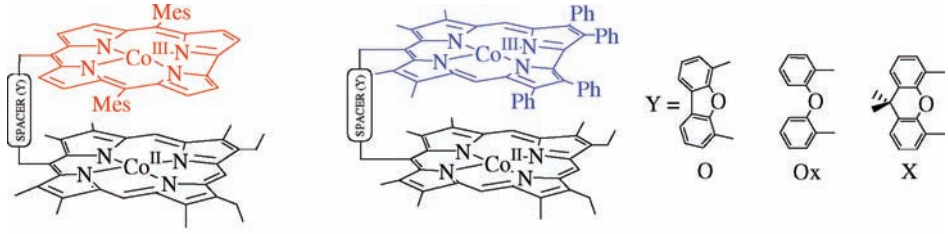

$(PMes_2CO)Co_2$ **(1)**
$(PMes_2COx)Co_2$ **(2)**
$(PMes_2CX)Co_2$ **(3)**

$(PCO)Co_2$ **(4)**
$(PCOx)Co_2$ **(5)**
$(PCX)Co_2$ **(6)**

phyrins[15−22] and corroles[23−25] have merited special attention as excellent functional cytochrome *c* oxidase models for the efficient catalytic reduction of oxygen to water.

Cobalt corroles have to date been the most well-characterized of the metallocorrole complexes.[23−32] In our own laboratories, we have examined the solution electrochemistry, spectroscopic properties, and axial ligand binding ability of mononuclear[24,26,31−36] and binuclear[24,37,38] cobalt(III) corroles with different macrocyclic structures. We also reported the electrochemistry and spectroscopic properties of dyads containing two face-to-face metallomacrocycles, one of which was a porphyrin and the other a corrole. Examples include dyads with a cobalt(III) corrole and a Co(II),[24,38,39] Fe(III),[23,40,41] Mn(III),[23,40,41] or free-base[25] porphyrin. In each case, the two macrocycles were linked to each other with a rigid spacer.

Mixed-valent dyads having a Co(II) porphyrin and Co(III) corrole linked by a dibenzofuran or 9,9-dimethylxanthene spacer were shown to be the efficient catalysts for the four-electron reduction of oxygen to water in acid media[23−25] while dyads with other linkers or those containing two cobalt(III) corroles[24] or one cobalt(III) corrole and a non-cobalt containing porphyrin[23,25,41] gave mainly H_2O_2 as the product of O_2 reduction. Measured half-wave potentials for the catalytic reduction of O_2 by four electrons ranged from 0.41 to 0.47 V versus the saturated calomel electrode (SCE)[24] while under the same solution conditions, the catalytic electroreduction of O_2 by two electrons to give H_2O_2 as a final product occurred at an average $E_{1/2}$ value of 0.34 V versus SCE.[23,41]

We earlier proposed[23] that these changes in potential for the electrocatalytic reduction of O_2 at an electrode surface, as well as differences in the number of electron transferred, 2 or 4, and the product of O_2 reduction, H_2O or H_2O_2, were all related to the initial site of electron transfer in the dyad, either at the cobalt central metal ion of the corrole or at the cobalt central metal ion of the porphyrin. This point is investigated in the present study where we have prepared a series of cofacial porphyrin-corrole dyads, **1**−**3**, (Chart 1) possessing a *meso*-substituted corrole macrocycle rather than

(14) Michel, H.; Behr, J.; Harrenga, A.; Kannt, A. *Annu. Rev. Biophys. Biomol. Struct.* **1998**, *27*, 329–356.
(15) Chang, C. J.; Loh, Z.-H.; Shi, C.; Anson, F. C.; Nocera, D. C. *J. Am. Chem. Soc.* **2004**, *126*, 10013–10020.
(16) Chang, C. J.; Deng, Y.; Shi, C.; Chang, C. K.; Anson, F. C.; Nocera, D. G. *Chem. Commun.* **2000**, 1355–1356.
(17) Collman, J. P.; Boulatov, R.; Sunderland, C. J.; Fu, L. *Chem. Rev.* **2004**, *104*, 561–588.
(18) Collman, J. P.; Fu, L.; Herrmann, P. C.; Zhang, X. *Science* **1997**, *275*, 949–951.
(19) Guilard, R.; Brandes, S.; Tardieux, C.; Tabard, A.; L'Her, M.; Miry, C.; Gouerec, P.; Knop, Y.; Collman, J. P. *J. Am. Chem. Soc.* **1995**, *117*, 11721–11729.
(20) Fukuzumi, S.; Okamoto, K.; Gros, C. P.; Guilard, R. *J. Am. Chem. Soc.* **2004**, *126*, 10441–10449.
(21) Fukuzumi, S.; Okamoto, K.; Tokuda, Y.; Gros, C. P.; Guilard, R. *J. Am. Chem. Soc.* **2004**, *126*, 17059–17066.
(22) (a) Collman, J. P.; Boulatov, R.; Sunderland, C. J. In *The Porphyrin Handbook*; Kadish, K. M., Smith, K. M., Guilard, R., Eds.; Academic Press: San Diego, CA, 2003; Vol. *11*, pp 1−50. (b) Rosenthal, J.; Nocera, D. G. In *Progress in Inorganic Chemistry*; Karlin, K. D., Ed.; John Wiley & Sons, Inc.: New York, 2007; Vol *55*, pp 483−544.
(23) Kadish, K. M.; Frémond, L.; Burdet, F.; Barbe, J.-M.; Gros, C. P.; Guilard, R. *J. Inorg. Biochem.* **2006**, *100*, 858–868.
(24) Kadish, K. M.; Frémond, L.; Ou, Z.; Shao, J.; Shi, C.; Anson, F. C.; Burdet, F.; Gros, C. P.; Barbe, J.-M.; Guilard, R. *J. Am. Chem. Soc.* **2005**, *127*, 5625–5631.
(25) Kadish, K. M.; Shao, J.; Ou, Z.; Frémond, L.; Zhan, R.; Burdet, F.; Barbe, J.-M.; Gros, C. P.; Guilard, R. *Inorg. Chem.* **2005**, *44*, 6744–6754.
(26) Kadish, K. M.; Shen, J.; Frémond, L.; Chen, P.; El Ojaimi, M.; Chkounda, M.; Gros, C. P.; Barbe, J.-M.; Ohkubo, K.; Fukuzumi, S.; Guilard, R. *Inorg. Chem.* **2008**, *47*, 6726–6737.
(27) Ramdhanie, B.; Telser, J.; Caneschi, A.; Zakharov, L. N.; Rheingold, A. L.; Goldberg, D. P. *J. Am. Chem. Soc.* **2004**, *126*, 2515–2525.
(28) Ramdhanie, B.; Zakharov, L. N.; Rheingold, A. L.; Goldberg, D. P. *Inorg. Chem.* **2002**, *41*, 4105–4107.
(29) Erben, C.; Will, S.; Kadish, K. M. In *The Porphyrin Handbook*; Kadish, K. M., Smith, K. M., Guilard, R., Eds.;Academic Press: San Diego, CA, 2000; Vol. 2, pp 233−300.
(30) Guilard, R.; Barbe, J.-M.; Stern, C.; Kadish, K. M. In *The Porphyrin Handbook*; Kadish, K. M., Smith, K. M., Guilard, R., Eds.; Academic Press: San Diego, CA, 2003; Vol. *18*, pp 303−349.
(31) Will, S.; Lex, J.; Vogel, E.; Adamian, V. A.; Van Caemelbecke, E.; Kadish, K. M. *Inorg. Chem.* **1996**, *35*, 5577–5583.
(32) Kadish, K. M.; Adamian, V. A.; Van Caemelbecke, E.; Gueletti, E.; Will, S.; Erben, C.; Vogel, E. *J. Am. Chem. Soc.* **1998**, *120*, 11986–11993.
(33) Kadish, K. M.; Koh, W.; Tagliatesta, P.; D'Souza, F.; Paolesse, R.; Licoccia, S.; Boschi, T. *Inorg. Chem.* **1992**, *31*, 2305–2313.
(34) Adamian, V. A.; D'Souza, F.; Licoccia, S.; Di Vona, M. L.; Tassoni, E.; Paolesse, R.; Boschi, T.; Kadish, K. M. *Inorg. Chem.* **1995**, *34*, 532–540.
(35) Guilard, R.; Gros, C. P.; Bolze, F.; Jérôme, F.; Ou, Z.; Shao, J.; Fischer, J.; Weiss, R.; Kadish, K. M. *Inorg. Chem.* **2001**, *40*, 4845–4855.
(36) Kadish, K. M.; Shao, J.; Ou, Z.; Gros, C. P.; Bolze, F.; Barbe, J.-M.; Guilard, R. *Inorg. Chem.* **2003**, *42*, 4062–4070.
(37) Guilard, R.; Jérôme, F.; Barbe, J.-M.; Gros, C. P.; Ou, Z.; Shao, J.; Fischer, J.; Weiss, R.; Kadish, K. M. *Inorg. Chem.* **2001**, *40*, 4856–4865.
(38) Kadish, K. M.; Ou, Z.; Shao, J.; Gros, C. P.; Barbe, J.-M.; Jérôme, F.; Bolze, F.; Burdet, F.; Guilard, R. *Inorg. Chem.* **2002**, *41*, 3990–4005.
(39) Guilard, R.; Jérôme, F.; Gros, C. P.; Barbe, J.-M.; Ou, Z.; Shao, J.; Kadish, K. M. C. R. *Acad. Sci., Serie IIc: Chimie* **2001**, *4*, 245–254.
(40) Guilard, R.; Burdet, F.; Barbe, J.-M.; Gros, C. P.; Espinosa, E.; Shao, J.; Ou, Z.; Zhan, R.; Kadish, K. M. *Inorg. Chem.* **2005**, *44*, 3972–3983.
(41) Kadish, K. M.; Shao, J.; Ou, Z.; Zhan, R.; Burdet, F.; Barbe, J.-M.; Gros, C. P.; Guilard, R. *Inorg. Chem.* **2005**, *44*, 9023–9038.

a β-pyrrole substituted corrole as was the case in earlier studies[24,38,39] where dyads **4** and **6** served as the catalysts. The same three linkers were used in both series, namely, dibenzofuran (O), diphenylether (Ox), or 9,9-dimethylxanthene (X).

Our intended goal in preparing the *meso*-substituted corroles in dyads **1**−**3** was to increase the Lewis acid character of the macrocycle to shift the formal Co^{III}/Co^{IV} process to a more positive potential and thus enhance the $4e^-$ reduction of dioxygen to water. Each newly synthesized compound was investigated by electrochemistry and spectroelectrochemistry to assign the site of electron transfer under different solution conditions.

Small changes in the macrocyclic substituents or linking group structure as well as differences in solvent axial coordination to one or both cobalt central metal ions of the dyad can lead to a major change in the site of electron transfer which would not be evident from measurements of redox potentials alone. This is especially the case for the first two one-electron abstractions involving the six dyads in Chart 1 where $E_{1/2}$ values for the formal Co^{III}/Co^{IV} reaction of the corrole and the Co^{II}/Co^{III} reaction of the porphyrin are quite close to each other, and a preferential "tuning" of which process occurs first can be easily accomplished by changing the position and/or type of corrole substituents, as well as the utilized electrochemical solvent. The potentials for oxidation of the Co(II) porphyrin and Co(III) corrole will also depend upon the gas above the solution. This is N_2 or Ar under usual electrochemical conditions but can be changed to carbon monoxide which is known to strongly bind with the Co(III) forms of both macrocycles but not to the Co(II) or Co(IV) forms of the compounds.[35,37,38,42,43]

Experimental Section

Chemicals and Compounds. Neutral alumina (Merck; usually Brockmann grade III, i.e., deactivated with 6% water) was used for column chromatography. Reactions were monitored by thin-layer chromatography and UV−visible spectroscopy. For electrochemical studies, absolute dichloromethane (CH_2Cl_2) was obtained from EMD Chemical Inc. and used without further purification while benzonitrile (PhCN) was purchased from Sigma-Aldrich Chemical Co. and distilled over P_2O_5 under reduced pressure prior to use. 1,1′-Dimethylferrocene (Aldrich Co., USA) was obtained commercially and purified by sublimation or recrystallization from ethanol. Tetra-*n*-butylammonium perchlorate (TBAP, Fluka Chemical Co.) was twice recrystallized from absolute ethanol and dried in a vacuum oven at 40 °C for 1 week prior to use. Perchloric acid ($HClO_4$, 70%) was purchased from Sigma-Aldrich Chemical Co. Aqueous solutions of 1 M $HClO_4$ were prepared with deionized water of resistivity not less than 18 MΩ cm. High purity N_2 gas was purchased from Matheson-Trigas.

Dyads **4** and **6** were synthesized as described in the literature.[44] The alkylporphyrin-*meso*-substituted-corroles $(PMes_2CY)H_5$ with Y = 9,9-dimethylxanthene (X) or dibenzofuran (O) used in this study were synthesized according to literature procedures.[45,46] Details for the synthesis and analytical data of the cobalt dyads are described below.

[5-(2,3,7,8,12,18-Hexamethyl-13,17-diethylporphyrin-5-yl)-4-(5,15-dimesitylcorrol-10-yl)-dibenzofuran]biscobalt $(PMes_2CO)Co_2$ (1). Under argon, a solution of 100 mg (0.087 mmol) of the free-base porphyrin-corrole dyad $(PMes_2CO)H_5$, 35 mg (0.145 mmol) of cobalt(II) acetate tetrahydrate in 10 mL of $CHCl_3$/methanol (70/30) was stirred and refluxed for 1 h 15 min, the metalation reaction being monitored by UV−visible spectroscopy and matrix-assisted laser desorption ionization/time of flight (MALDI/TOF) mass spectrometry. The solution was then poured in water (100 mL) and extracted with dichloromethane. The combined organic layers were dried over $MgSO_4$. After removal of the solvent in vacuo, the residue so obtained was redissolved in dichloromethane and chromatographed on alumina using CH_2Cl_2 as eluent. The title product **1** was isolated in 41% yield (45 mg; 0.037 mmol). MS (MALDI/TOF): m/z = 1261.58 $[M]^{+\bullet}$; 1261.41 calcd for $C_{79}H_{67}N_8OCo_2$. UV−vis (CH_2Cl_2): λ_{max} ($\varepsilon \times 10^{-3}$ M^{-1} cm^{-1}) = 394.1 (97.2), 525.0 (9.7), 555.0 (11.0) nm. Anal. Calcd for $C_{79}H_{67}N_8OCo_2$: C, 75.17; H, 5.35; N, 8.88. Found: C, 74.93; H, 5.01; N, 8.59.

[2-(2,3,7,8,12,18-Hexamethyl-13,17-diethylporphyrin-5-yl)-2′-(5,15-dimesitylcorrol-10-yl)diphenylether]biscobalt $(PMes_2COx)Co_2$ (2). This compound was synthesized as described above for **1**, starting from $(PMes_2COx)H_5$ (140 mg, 0.122 mmol, 1 equiv) in 53% yield (82 mg, 0.065 mmol). MS (MALDI/TOF): m/z = 1263.76 $[M]^{+\bullet}$; 1263.43 calcd for $C_{79}H_{69}N_8OCo_2$. UV−vis (CH_2Cl_2): λ_{max} ($\varepsilon \times 10^{-3}$ M^{-1} cm^{-1}) = 395.0 (93.8), 521.0 (9.2), 554.0 (10.2) nm. Anal. Calcd for $C_{79}H_{69}N_8OCo_2$: C, 75.05; H, 5.50; N, 8.86. Found: C, 74.87; H, 5.28; N, 8.69.

[5-(2,3,7,8,12,18-Hexamethyl-13,17-diethylporphyrin-5-yl)-4-(5,15-dimesitylcorrol-10-yl)-9,9-dimethylxanthene]biscobalt $(PMes_2CX)Co_2$ (3). This compound was synthesized as described above for **1**, starting from $(PMes_2CX)H_5$ (140 mg, 0.117 mmol, 1 equiv) in 37% yield (56 mg, 0.043 mmol). MS (MALDI/TOF): m/z = 1303.20 $[M]^{+\bullet}$; 1303.46 calcd for $C_{82}H_{73}N_8OCo_2$. UV−vis (CH_2Cl_2): λ_{max} ($\varepsilon \times 10^{-3}$ M^{-1} cm^{-1}) = 388.9 (94.1), 524.0 (9.5), 558.0 (11.0) nm. Anal. Calcd for $C_{82}H_{73}N_8OCo_2$: C, 75.51; H, 5.64; N, 8.59. Found: C, 75.37; H, 5.29; N, 8.27.

2-[(5,5′-Diethoxycarbonyl-3,3′,4,4′-tetramethyl-2,2′-dipyrryl)-methyl]-2′-(13,17-diethyl-2,3,7,8,12,18-hexamethylporphyrin-5-yl)diphenylether. Under nitrogen, a mixture of monoformyl diphenylether porphyrin[46] (1.62 g, 2.5 mmol, 1 equiv) and 2-ethoxycarbonyl-3,4-dimethylpyrrole (0.92 g, 5.5 mmol, 2.2 equiv) was dissolved in 110 mL of hot ethanol. Hydrochloric acid (4 mL, 45.9 mmol) was then added, and the mixture was stirred under reflux for 4 h. The mixture was cooled down, and the solvent removed under vacuum. The residue was dissolved in dichloromethane and washed with water. The organic layers were dried over $MgSO_4$, filtered, and evaporated under vacuum. After purification on silica (CH_2Cl_2), the title compound was isolated in 77% yield (1.89 g, 1.96 mmol) as purple crystals. ^1H NMR ($CDCl_3$) δ (ppm): 10.12 (s, 2H, CH_{meso}), 9.95 (s, 1H, CH_{meso}), 8.49 (br s, 2H, NH), 7.95 (dd, 1H, $^3J_{H-H}$ = 7.3 Hz, $^4J_{H-H}$ = 1.5 Hz, Ar−H), 7.68 (td, 1H, $^3J_{H-H}$ = 8.0 Hz, $^4J_{H-H}$ = 1.5 Hz, Ar−H), 7.45 (t, 1H, $^3J_{H-H}$ = 7.5 Hz, Ar−H), 7.33 (d, 1H, $^3J_{H-H}$ = 8.0 Hz, Ar−H), 7.27 (d, 1H, $^3J_{H-H}$ = 7.4 Hz, Ar−H), 7.19 (td, 1H, $^3J_{H-H}$ = 7.9 Hz, $^4J_{H-H}$ = 1.4 Hz, Ar−H), 6.80 (t, 1H, $^3J_{H-H}$ = 7.5 Hz, Ar−H), 6.50 (d, 1H,

(42) Mu, X. H.; Kadish, K. M. *Inorg. Chem.* **1989**, *28*, 3743–3747.
(43) Kadish, K. M.; Li, J.; Van Caemelbecke, E.; Ou, Z.; Guo, N.; Autret, M.; D'Souza, F.; Tagliatesta, P. *Inorg. Chem.* **1997**, *36*, 6292–6298.
(44) Barbe, J.-M.; Burdet, F.; Espinosa, E.; Gros, C. P.; Guilard, R. *J. Porphyrins Phthalocyanines* **2003**, *7*, 365–374.
(45) Barbe, J.-M.; Burdet, F.; Espinosa, E.; Guilard, R. *Eur. J. Inorg. Chem.* **2005**, 1032–1041.
(46) Gros, C. P.; Brisach, F.; Meristoudi, A.; Espinosa, E.; Guilard, R.; Harvey, P. D. *Inorg. Chem.* **2007**, *46*, 125–135.

$^3J_{H-H}$ = 7.3 Hz, Ar−H), 5.85 (s, 1H, CH), 4.07 (q, 4H, $^3J_{H-H}$ = 7.7 Hz, CH_2-CH_3), 4.01 (q, 4H, $^3J_{H-H}$ = 7.1 Hz, CH_2-CH_3), 3.63 (s, 6H, CH_3), 3.53 (s, 6H, CH_3), 2.54 (s, 6H, CH_3), 1.88 (t, 6H, $^3J_{H-H}$ = 7.7 Hz, CH_2-CH_3), 1.67 (s, 6H, CH_3), 1.11 (t, 6H, $^3J_{H-H}$ = 7.1 Hz, CH_2-CH_3), 0.44 (s, 6H, CH_3), −3.16 (br s, 1H, NH), −3.30 (br s, 1H, NH). MS (MALDI/TOF): m/z = 962.31 $[M]^{+\bullet}$; 962.51 calcd for $C_{61}H_{66}N_6O_5$. UV−vis (CH_2Cl_2): λ_{max} ($\varepsilon \times 10^{-3}$ M^{-1} cm^{-1}) = 403 (185), 501 (17.4), 535 (8.6), 572 (6.6), 626 (2.7). Anal. Calcd for $C_{61}H_{66}N_6O_5$: C, 76.06; H, 6.91; N, 8.72. Found: C, 75.82; H, 7.05; N, 8.53.

2-[(3,3′,4,4′-Tetramethyl-2,2′-dipyrryl)methyl]-2′-(13,17-diethyl-2,3,7,8,12,18-hexamethylporphyrin-5-yl)diphenylether. A suspension of 1.55 g of 2-[(5, 5′-diethoxycarbonyl-3, 3′, 4, 4′-tetramethyl-2, 2′-dipyrryl)methyl]-2′-(13, 17-diethyl-2, 3, 7, 8, 12, 18-hexamethylporphyrin-5-yl) diphenylether (1.61 mmol) in diethylene glycol (120 mL) containing NaOH (1.9 g) was heated at 110 °C under N_2 for 1 h 30 min and then at 190 °C for another 1 h 30 min after which the mixture was poured into ice water (2000 mL), and the resulting solid was filtered, washed thoroughly with water, and then dried under vacuum to give the title compound (1.21 g, 1.48 mmol, 92%). ^{1}H NMR ($CDCl_3$) δ (ppm): 10.14 (s, 2H, CH_{meso}), 9.98 (s, 1H, CH_{meso}), 8.52 (s, 2H, NH), 7.98 (dd, 1H, $^3J_{H-H}$ = 7.3 Hz, $^4J_{H-H}$ = 1.5 Hz, Ar−H), 7.72 (td, 1H, $^3J_{H-H}$ = 8.0 Hz, $^4J_{H-H}$ = 1.5 Hz, Ar−H), 7.48 (t, 1H, $^3J_{H-H}$ = 7.5 Hz, Ar−H), 7.36 (d, 1H, $^3J_{H-H}$ = 8.0 Hz, Ar−H), 7.29 (d, 1H, $^3J_{H-H}$ = 7.4 Hz, Ar−H), 7.21 (td, 1H, $^3J_{H-H}$ = 7.9 Hz, $^4J_{H-H}$ = 1.4 Hz, Ar−H), 6.83 (t, 1H, $^3J_{H-H}$ = 7.5 Hz, Ar−H), 6.52 (d, 1H, $^3J_{H-H}$ = 7.3 Hz, Ar−H), 5.86 (s, 1H, CH), 4.11 (q, 4H, $^3J_{H-H}$ = 7.1 Hz, CH_2-CH_3), 3.67 (s, 6H, CH_3), 3.58 (s, 6H, CH_3), 3.45 (s, 6H, CH_3), 1.86 (s, 6H, CH_3), 1.62 (t, 6H, $^3J_{H-H}$ = 7.1 Hz, CH_2-CH_3), 0.48 (s, 6H, CH_3), −2.86 (br s, 1H, NH), −3.01 (br s, 1H, NH). MS (MALDI/TOF): m/z = 818.53 $[M]^{+\bullet}$; 818.47 calcd for $C_{55}H_{58}N_6O$. HR-MS (MALDI/TOF): m/z = 818.4701 $[M]^{+\bullet}$; 818.4672 calcd for $C_{55}H_{58}N_6O$. UV−vis (CH_2Cl_2): λ_{max} ($\varepsilon \times 10^{-3}$ M^{-1} cm^{-1}) = 399 (332), 507 (27.4), 539 (20.4), 576 (25.1), 608 (15.6).

2-(2,3,7,8,12,18-Hexamethyl-13,17-diethylporphyrin-5-yl)-2′-(7,8,12,13-tetramethyl-2,3,17,18-tetraphenylcorrol-10-yl)diphenylether, (PCOx)H$_5$. Under argon, a mixture of 2-(2,3,7,8,12,18-hexamethyl-13,17-diethylporphyrin-5-yl)-2′-((3,3′,4,4′-tetramethyldipyrryl)-methyl)diphenylether (850 mg, 1.04 mmol, 1 equiv) and 2-formyl-3,4-diphenylpyrrole[35] (565 mg, 2.49 mmol, 2.4 equiv) was refluxed in 500 mL of methanol. Hydrobromic acid 33% wt in glacial acetic acid (5.70 mL, 31.0 mmol, 30 equiv) was then added, and the resulting red mixture was refluxed for 15 min. Sodium acetate trihydrate (39.6 g, 291 mmol, 280 equiv) was added and, after refluxing for 5 min, the reaction mixture was allowed to cool down to 0 °C by the use of an ice-bath. Water was added to complete the precipitation. After filtration of the precipitate, the dark solid was dissolved in CH_2Cl_2 (300 mL). A solution of *p*-chloranil (511 mg, 2.08 mmol, 2 equiv) in toluene (20 mL) was added and the mixture was stirred for 5 min. Hydrazine monohydrate (0.9 mL, 18.7 mmol, 9 equiv) was then added and the mixture stirred again for 5 min. The organic layer was washed three times with 300 mL of water, dried over $MgSO_4$, and the solvent was evaporated. The solid was chromatographed on basic alumina (CH_2Cl_2 as eluent), and the first dark band was collected to give the title porphyrin-corrole dyad (PCOx)H$_5$ which was recrystallized from CH_2Cl_2/MeOH (545 mg, 0.43 mmol, 41%). ^{1}H NMR ($CDCl_3$) δ (ppm): 9.93 (s, 2H, C*H*), 9.36 (s, 1H, C*H*), 8.83 (s, 2H, C*H*), 7.88 (dd, 1H, $^3J_{H-H}$ = 7.3 Hz, $^4J_{H-H}$ = 1.5 Hz, Ar−H), 7.61 (td, 1H, $^3J_{H-H}$ = 8.0 Hz, $^4J_{H-H}$ = 1.5 Hz, Ar−H), 7.41 (m, 5H, Ph*H*), 7.36 (t, 1H, $^3J_{H-H}$ = 7.5 Hz, Ar−H), 7.33 (m, 5H, Ph*H*), 7.28 (m, 5H, Ph*H*), 7.26 (d, 1H, $^3J_{H-H}$ = 8.0 Hz, Ar−H), 7.21 (d, 1H, $^3J_{H-H}$ = 7.4 Hz, Ar−H), 7.14 (td, 1H, $^3J_{H-H}$ = 7.9 Hz, $^4J_{H-H}$ = 1.4 Hz, Ar−H), 7.01−6.81 (m, 5H, Ph*H*), 6.78 (t, 1H, $^3J_{H-H}$ = 7.5 Hz, Ar−H), 6.46 (d, 1H, $^3J_{H-H}$ = 7.3 Hz, Ar−H), 4.04 (dq, $^2J_{HA-HB}$ = 15.2 Hz, $^3J_{H-H}$ = 7.9 Hz, 2H, CH_AH_B-CH_3), 3.85 (dq, $^2J_{HA-HB}$ = 15.1 Hz, $^3J_{H-H}$ = 7.8 Hz, 2H, CH_AH_B-CH_3), 3.24 (s, 6H, CH_3), 2.95 (s, 6H, CH_3), 2.49 (s, 6H, CH_3), 1.84 (s, 6H, CH_3), 1.57 (t, $^3J_{H-H}$ = 7.9 Hz, 3H, CH_2-CH_3), 1.54 (t, $^3J_{H-H}$ = 7.8 Hz, 3H, CH_2-CH_3), 1.39 (s, 6H, CH_3), −4.11 ppm (s, 2H, N*H*), −4.19 (s, 3H, N*H*). MS (MALDI/TOF): m/z = 1274.63 $[M]^{+\bullet}$; 1274.50 calcd for $C_{89}H_{78}N_8O$. HR-MS (MALDI/TOF): m/z = 1274.6327 $[M]^{+\bullet}$; 1274.6299 calcd for $C_{89}H_{78}N_8O$. UV−vis (CH_2Cl_2): λ_{max} ($\varepsilon \times 10^{-3}$ M^{-1} cm^{-1}) = 399 (332), 507 (27.4), 539 (20.4), 576 (25.1), 608 (15.6).

[2-(2,3,7,8,12,18-Hexamethyl-13,17-diethylporphyrin-5-yl)-2′-(7,8,12,13-tetramethyl-2,3,17,18-tetraphenylcorrol-10-yl)-diphenylether]biscobalt, (PCOx)Co$_2$ (5). This compound was synthesized as described above for **1**, starting from (PCOx)H$_5$ (170 mg, 0.13 mmol, 1 equiv) in 49% yield (90 mg, 0.065 mmol). MS (MALDI/TOF): m/z = 1387.38 $[M]^{+\bullet}$; 1387.46 calcd for $C_{89}H_{73}N_8OCo_2$. HR-MS (MALDI/TOF): m/z = 1387.4602 $[M]^{+\bullet}$; 1387.4571 calcd for $C_{89}H_{73}N_8OCo_2$. UV−vis (CH_2Cl_2): λ_{max} ($\varepsilon \times 10^{-3}$ M^{-1} cm^{-1}) = 393 (163.9), 530 (17.4), 557 (17.6).

Instrumentation

^{1}H NMR spectra were recorded on a Bruker DRX-500 AVANCE transform spectrometer at the "Centre de Spectrométrie Moléculaire de l'Université de Bourgogne"; chemical shifts are expressed in ppm relative to chloroform (7.258 ppm). Microanalyses were performed at the Université de Bourgogne on a Fisons EA 1108 CHNS instrument. UV−visible spectra were recorded on a Varian Cary 1 spectrophotometer. Mass spectra and accurate mass measurements (HR-MS) were obtained on a Bruker Daltonics Ultraflex II spectrometer of the "Centre de Spectrométrie Moléculaire" in the MALDI/TOF reflectron mode using dithranol as a matrix. Cyclic voltammetry was carried out with an EG&G model 173 potentiostat/galvanostat. A three-electrode system was used and consisted of a glassy carbon or a platinum disk working electrode, a platinum wire counter electrode, and a saturated calomel reference electrode (SCE). The SCE electrode was separated from the bulk of the solution by a fritted-glass bridge of low porosity, which contained the solvent/supporting electrolyte. Half-wave potentials for reversible redox processes were determined by cyclic voltammetry and were calculated as $E_{1/2} = (E_{pa} + E_{pc})/2$ where E_{pa} and E_{pc} represent the anodic and cathodic peak potentials, respectively.

The measurement of the O_2 reduction activity of the cobalt complexes were carried out using a three electrode system consisting of a platinum ring-graphite disk working electrode (Model MTI34, Pine Instruments Co.), a platinum wire as the auxiliary electrode, and a SCE electrode which was separated from the bulk of the solution by means of a salt bridge. The rotating ring-disk electrode, purchased from the Pine Instrument Co., consisted of a platinum ring and a removable edge-plane pyrolytic graphite (EPPG) disk (A = 0.282 cm^2). Cyclic and rotating disk voltammograms were carried out using a Pine model AFMSR rotator linked to an EG&G Princeton Applied Research (PAR) model 263A

Table 1. Half-Wave Potentials (V vs SCE) and Proposed Site of Electron Transfer for Dyads **1**−**6** and Monomacrocycles **7**-**9** in PhCN Containing 0.1 M TBAP

	proposed site of oxidation						proposed site of reduction		
compound	Cor	Por	Cor	Por	Cor	Por	Cor	Por	Cor
$(PMes_2CO)Co_2$ (**1**)	1.61	1.25	0.98[a]	0.98[a]	0.57	0.41	−0.16	−1.06	−1.75
$(PMes_2COx)Co_2$ (**2**)	1.66	1.24	1.01	0.89	0.53	0.38	−0.21	−1.13	−1.79
$(PMes_2CX)Co_2$ (**3**)		1.25	0.95[a]	0.95[a]	0.55	0.44	−0.26	−1.19	−1.90[b]
$(PCO)Co_2$[d] (**4**)		1.25	0.96	0.87	0.39	0.47	−0.19	−1.02	−1.64
$(PCOx)Co_2$ (**5**)	1.35	1.16	1.04	0.83	0.45	0.52	−0.29	−1.15[c]	−1.75
$(PCX)Co_2$ (**6**)		1.30	0.98[a]	0.98[a]	0.38		−0.39	−1.09	
$(Me_6Et_2PhPor)Co$[d] (**7**)		1.25		1.01		0.36		−1.08	
$(F_5PhMes_2Cor)Co$[e] (**8**)	1.70		1.00		0.57		−0.07		−1.68
$(Me_4Ph_5Cor)Co$[f] (**9**)	1.45[b]		0.82		0.47		−0.16		−1.67

[a] Overlapping one-electron transfer processes at the same potential. [b] Peak potential at a scan rate of 0.1 V/sec. [c] Extra reduction was observed at $E_{1/2}$ = −1.02 V. [d] Data taken from ref 38. [e] Data taken from ref 26. [f] Data taken from ref 36.

potentiostat/galvanostat. The potentiostat was controlled by an IBM compatible PC microcomputer having an M270 (EG&G PARC) software package.

UV−visible spectroelectrochemical experiments were performed with an optically transparent platinum thin-layer electrode of the type described in the literature.[47] Potentials were applied with an EG&G PAR model 173 potentiostat. Time-resolved UV−visible spectra were recorded with a Hewlett-Packard Model 8453 diode array rapid-scanning spectrophotometer.

Electrode Surface Preparation for O_2 Catalysis

Before use, the edge-plane pyrolytic graphite with the edges of the graphitic planes exposed was polished with 600 grit SiC paper, rinsed with purified water, and wiped off with clean tissue before it was coated with the catalytic film. The catalysts were adsorbed onto the graphite disk by transferring aliquots of a solution in $CHCl_3$ directly to the electrode surface followed by evaporation of the solvent. Potentials were measured with respect to a saturated calomel reference electrode (SCE).

The slopes of the diagnostic Koutecky−Levich plots were determined by linear regression analysis of data acquired at 100, 300, 600, 900, 1600, 2500, and 3600 rpm (rpm = rotation per minute). The diffusion-limiting currents for the reduction of O_2 in aqueous solution at the rotating disk electrode were calculated using the following parameters: kinematic viscosity of H_2O at 25 °C, 0.01 $cm^2\ s^{-1}$; solubility of O_2 in air-saturated 1 M $HClO_4$, 0.24 mM; diffusion coefficient of O_2, 1.7×10^{-5} $cm^2\ s^{-1}$.[48]

Homogeneous catalytic reduction of oxygen by 1,1′-dimethylferrocene $Fe(C_5H_4Me)_2$ in the presence of $HClO_4$ and the biscobalt cofacial porphyrin-corrole dyads was examined by monitoring the appearance of an absorption band due to $[Fe(C_5H_4Me)_2]^+$ (λ_{max} = 650 nm, ε_{max} = 290 $M^{-1}\ cm^{-1}$)[49] using a Hewlett-Packard 8453 diode array spectrophotometer with a quartz cuvette (path length = 10 mm) at 298 K. An air-saturated PhCN solution was used for the catalytic reduction of oxygen by $Fe(C_5H_4Me)_2$. The O_2 concentration in an air-saturated PhCN solution (1.7×10^{-3} M) was determined as reported in the literature.[50] The concentrations of $Fe(C_5H_4Me)_2$ used for the catalytic reduction of O_2 were larger than the O_2 concentration in solution so that oxygen was the limiting reagent in the reaction cell which was filled with the reactant solution.

Results and Discussion

Electrochemistry of Biscobalt Porphyrin-Corrole Dyads in PhCN. Each dyad in PhCN containing 0.1 M TBAP exhibits three reductions and five or six oxidations between +1.9 and −1.9 V versus SCE. The measured $E_{1/2}$ values are summarized in Table 1 under the proposed site of electron transfer which is listed as "Cor" and "Por" for corrole- and porphyrin-centered redox reaction, respectively.

Site of Electroreduction in the Dyads. The sites of electron transfer indicated in Table 1 for the three one-electron *reductions* of **1**−**6** are easily assigned by comparison with potentials reported in the literature for reduction of numerous Co(III) corroles and Co(II) porphyrins over the last four decades.[20,21,29,30,51] This contrasts with the electrooxidation where a definitive site of electron abstraction from the dyads cannot be done on the basis of redox potentials alone. In this case, the use of spectroelectrochemistry is needed along with a comparison between the electrochemistry of dyads **1**−**6** and that of structurally related monomeric porphyrins or corroles **7–9** such as those shown in Chart 2 which were previously characterized in detail.[26,36,38]

The first reduction of monomeric Co(III) corroles leads to a Co(II) complex and generally occurs at $E_{1/2}$ values between 0.13 to −0.36 V versus SCE in PhCN, the exact potential depending upon the macrocyclic structure and presence of any axial ligand.[26,29,33,36] A second electron can then be added to the singly reduced corrole at $E_{1/2}$ values between −1.40 and −1.75 V, and this reaction leads either to a Co(II) corrole π-anion radical or a Co(I) corrole with an uncharged macrocyclic ring as has been assigned in many cases.[26,29,52]

(47) Lin, X. Q.; Kadish, K. M. *Anal. Chem.* **1985**, *57*, 1498–1501.
(48) Shi, C.; Anson, F. C. *Inorg. Chem.* **1998**, *37*, 1037–1043.
(49) Fukuzumi, S.; Mochizuki, S.; Tanaka, T. *Inorg. Chem.* **1989**, *28*, 2459–2465.
(50) Fukuzumi, S.; Ishikawa, M.; Tanaka, T. *J. Chem. Soc., Perkin Trans. 2* **1989**, 1037–1045.
(51) Kadish, K. M.; Van Caemelbecke, E.; Royal, G. In *The Porphyrin Handbook*; Kadish, K. M., Smith, K. M., Guilard, R., Eds.; Academic Press: San Diego, CA, 2000; Vol. 8, pp 1−114.
(52) Grodkowski, J.; Neta, P.; Fujita, E.; Mahammed, A.; Simkhovich, L.; Gross, Z. *J. Phys. Chem. A* **2002**, *106*, 4772–4778.

Chart 2. Monomeric Macrocycles Used for Comparison to Dyads

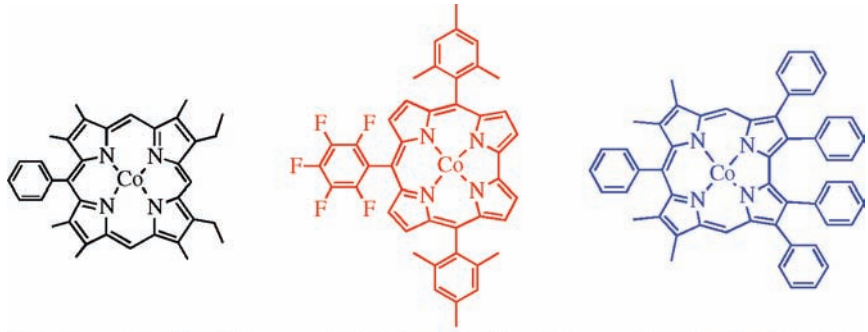

Scheme 1. Reduction of Dyads **1**−**6**

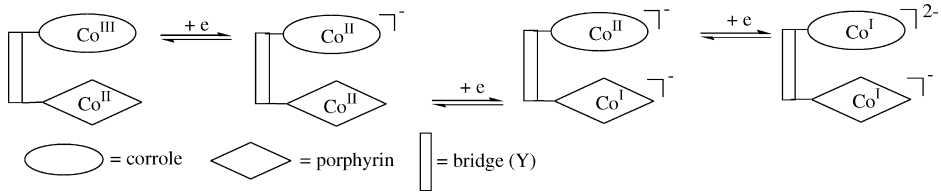

Under the same solution conditions, monomeric Co(II) porphyrins are generally reduced to their Co(I) form at potentials between −0.60 and −1.00 V versus SCE, with $E_{1/2}$ values for this process depending mainly on the structure and electron-donating or electron-withdrawing substituents of the macrocycle.[51] These electrode reactions vary little with changes in solvent or supporting electrolyte, in large part because the Co^{I} porphyrin does not bind axial ligands and the Co^{II} complex does so only weakly.[51] Because of what we already know from the literature,[38,41] there can be little doubt when assigning each reduction of **1**−**6** to a specific macrocycle. The first and third reductions of these dyads are corrole-centered while the second reduction involves the porphyrin macrocycle as schematically illustrated in Scheme 1 where the sequence of steps in the addition of three electrons can be described as Cor, Por, and Cor.

As seen in Table 1, small but significant differences in half-wave potentials are observed between each "Cor" or "Por" reduction of the dyads **1**−**6** and the same electrode reactions in the unlinked macrocycles, **7**, **8** or **9**. This is discussed on the following pages and is related to the degree of interaction between the two macrocycles of each dyad held together in a face-to-face arrangement by one of the three spacers shown in Chart 1.

Figure 1 compares cyclic voltammograms (CVs) of two dyads (**2** and **5**) and three monomeric macrocycles (**8**, **7** and **9**) in PhCN. Dyad **2** possesses a *meso*-substituted corrole while dyad **5** possesses a *β*-pyrrole substituted corrole (see Chart 1). The monomeric corrole **8** whose CV is shown in the upper box of Figure 1 is structurally related to the dyad **2** while the monomeric corrole **9** whose CV is in the lower box of Figure 1 is structurally related to the dyad **5**. The same cobalt(II) porphyrin **7** is found in both dyads **2** and **5**, and the CV of this compound is shown in the middle of the figure between CVs of two dyads.

A key piece of information which can be obtained from the voltammograms in Figure 1 is the interaction which

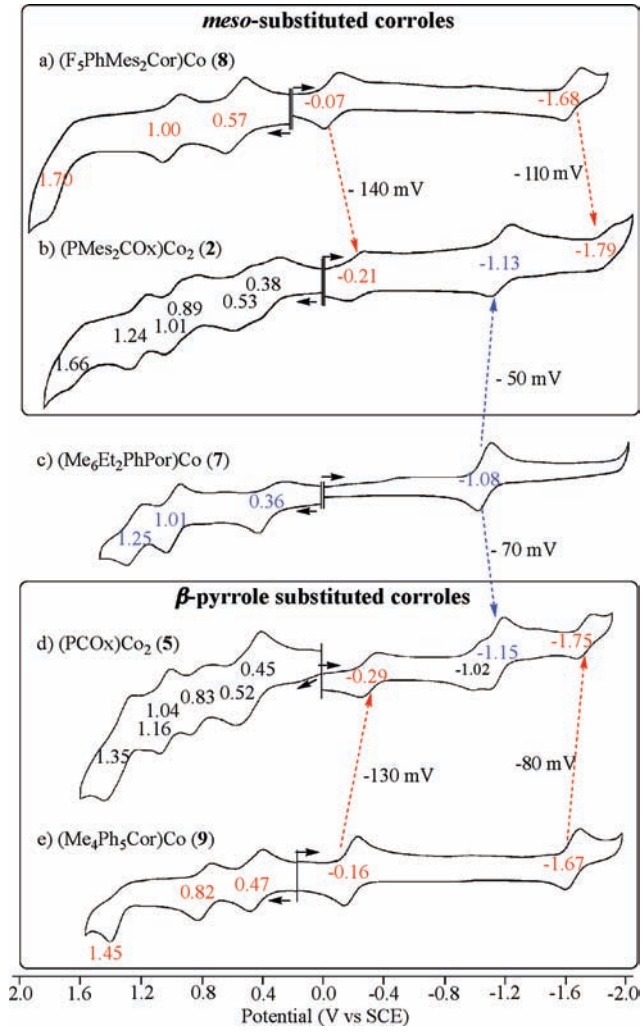

Figure 1. CVs of dyads **2** and **5** along with the structurally related monomacrocycles **8**, **7**, and **9** in PhCN containing 0.1 M TBAP. The top box contains CVs for compounds with *meso*-substituted corroles, and the lower has those with *β*-pyrrole substituted corroles. Both dyads have the same porphyrin macrocycle which is represented by compound **7**.

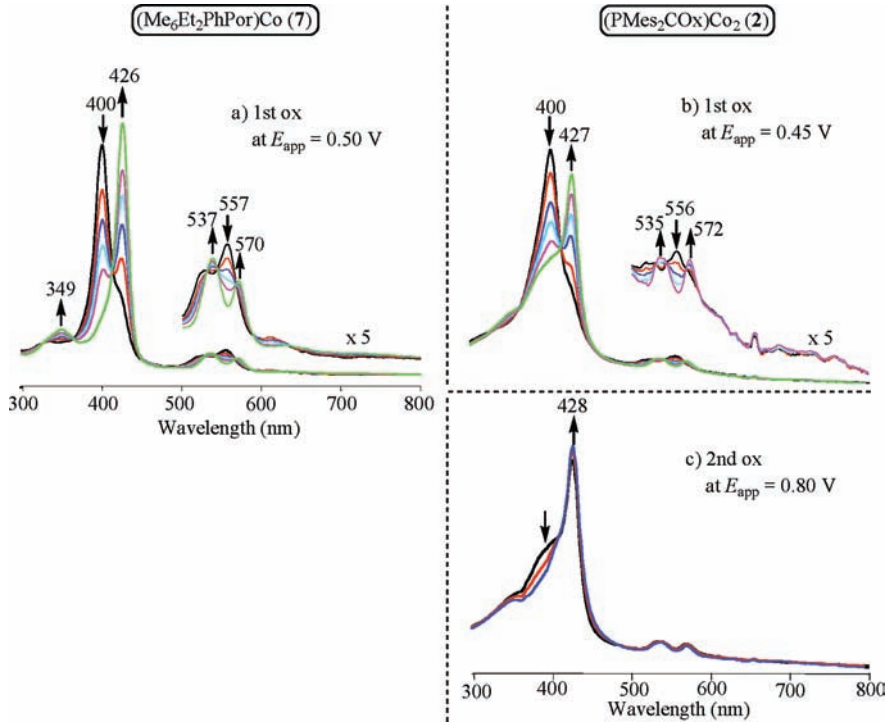

Figure 2. UV−visible spectral changes of complex **7** during the first oxidation (a) and **2** during the first (b) and second oxidation (c) in PhCN containing 0.1 M TBAP.

occurs between the two linked macrocycles in the cofacial dyad. Since, as indicated above, the site of each electron addition (corrole or porphyrin) is unambiguous, the magnitude of the interaction between the two macrocycles can be related to differences in half-wave potentials between reductions involving the dyad and the same electron transfer processes involving the unlinked corrole or unlinked porphyrin macrocycle. The difference in $E_{1/2}$ between a given reduction of the two compounds, monomer and dyad, is shown by arrows in Figure 1 and indicates both the direction and magnitude of the potential shift upon going from the monomer to the dyad, for example −130 mV and −80 mV between the first two one-electron reductions of **9** and the same redox processes of **5**.

A similar shift in $E_{1/2}$ is seen when comparing the redox reactions of **8** and **2**. The first reduction of the monocorrole **8** is located at $E_{1/2} = -0.07$ V (Figure 1a) which is 140 mV more positive than the $E_{1/2}$ of −0.21 V for the same metal-centered reduction of the porphyrin-corrole dyad **2** (Figure 1b). The much easier Co^{III}/Co^{II} reaction of the monocobalt corrole as compared to the related dyad might at first be attributed to the strong electron-withdrawing effect of the pentafluorophenyl group on compound **8** but as seen in the lower part of the figure, a similar −130 mV shift in $E_{1/2}$ is observed between the corrole Co^{III}/Co^{II} reaction of **9** and **5**, both of which are almost identical corrole structures and lack the C_6F_5 group of compound **8**. A negative 110 mV shift in $E_{1/2}$ is seen between the Co^{II}/Co^{I} reaction of the corrole upon going from the monocorrole **8** to the dyad **2,** and this compares to an −80 mV shift upon going from the monocorrole **9** to the dyad **5**. Again, the similar shifts in potentials suggest that there is a negligible substituent effect of the C_6F_5 group on both metal-centered reactions, and the difference in $E_{1/2}$ can then be attributed to a π-π interaction between the two macrocycles which makes the metal-centered corrole reduction more difficult in the dyad.

Shifts in the porphyrin centered redox processes toward more difficult reduction are also seen upon going from the monomeric macrocycle to the dyad. For example, the Co(II)/Co(I) reaction on the porphyrin unit in dyad **2** occurs at $E_{1/2} = -1.13$ V (Figure 1b) as compared to the Co(II)/Co(I) reaction of the monoporphyrin **7** which is located at $E_{1/2} = -1.08$ V (Figure 1c). This shift of $E_{1/2}$ may be due to π-π interaction between the two macrocycles, but it can also be due to the added negative charge on the dyad which undergoes the porphyrin-centered redox reaction. Since the corrole unit of the dyad **2** is reduced in the first step, the added negative charge will be felt by the porphyrin unit of the dyad which is harder to reduce by 50 mV as compared to the monoporphyrin. In a similar manner, the porphyrin Co^{II}/Co^{I} reaction of the dyad **5** is more difficult by 70 mV as compared to the same redox reaction of the monoporphyrin **7**.

The electroreduction behavior of dyads **1**, **3**, **4**, and **6** is similar to that for the dyads **2** or **5** in Figure 1, and the proposed electron-transfer mechanisms for these six dyads in nonaqueous solvents are as shown in Scheme 1 where the singly reduced species is assigned as $[(Por)Co(II)\text{-}(Cor)Co(II)]^{-}$, the doubly reduced species as $[(Por)Co(I)\text{-}(Cor)Co(II)]^{2-}$, and the triply reduced species as $[(Por)Co(I)\text{-}(Cor)Co(I)]^{3-}$. An additional reduction is also seen at −1.02 V for **5** but has not been assigned.

Spectroelectrochemistry to Assign Site of Electrooxidation in Dyads. The monoporphyrin **7** and the two monocorroles **8** and **9** each undergo three one-electron oxidations in PhCN containing 0.1 M TBAP, and the same reactions are seen in the porphyrin-corrole dyads where six closely spaced oxidation processes are observed as shown in Figure 1 for the case of **2** and **5**. A site of electron abstraction can be tentatively proposed for each oxidation of the dyads by comparing half-wave potentials for the linked and unlinked macrocycles in Figure 1 with what is known in the literature[26,29,38,41] for related compounds, but a definitive assignment would need spectroscopic verification because the first two oxidations of **2** and **5** have similar $E_{1/2}$ values, one of which involves the Co^{II}/Co^{III} process of the porphyrin and the other the formal Co^{III}/Co^{IV} reaction of the corrole. The key question we wish to answer is which process comes first, and to do this, an evaluation of the UV−visible spectra after each electron transfer is needed.

The UV−visible spectrum of each porphyrin-corrole dyad is, in part, a composite of spectra of the two conjugated macrocycles, but the molar absorptivity of the porphyrin bands is about 10 times larger than that of the corrole bands.[30] Thus, when the electron transfer reaction is located at the porphyrin part of the dyad, the Soret region of the UV−visible spectrum should undergo large changes in intensity, but only small changes in the Soret band region of the spectrum should be observed when an electron is abstracted or added at the corrole part of the dyad since the more intense porphyrin absorptions will still predominate. This is illustrated in Figure 2 which presents an example of how spectroelectrochemistry can be used to assign the initial site of oxidation for the case of **2** and **7** in PhCN. The metal-centered oxidation of **7** is located at 0.36 V in PhCN (Figure 1c) and is followed by two ring-centered reactions at $E_{1/2}$ = 1.01 and 1.25 V giving a Co^{III} π-cation radical and dication.[51] The initial Co^{II} form of the porphyrin **7** has a Soret band at 400 nm and a single visible band at 557 nm in PhCN while the Co^{III} oxidation product has a Soret band at 426 nm and two Q bands at 537 and 570 nm under the same solution conditions. Clear isosbestic points are seen for the Co^{II}/Co^{III} process of the monoporphyrin **7** upon application of an oxidizing potential, and these spectral changes are shown in Figure 2a.

Very similar spectral changes are seen upon oxidation of the dyad **2** at 0.45 V. These spectral changes are shown in Figure 2b and give a product with a Soret band at 427 nm and two Q bands at 535 and 572 nm. The first oxidation potential of **2** (0.38 V) and **7** (0.36 V) are also quite similar to each other, leaving little doubt that the first one-electron abstraction from the dyad involves the porphyrin and not the corrole part of the molecule. Thus, the first one-electron oxidized product of the dyad **2** is assigned as $[(Por)Co(III)\text{-}(Cor)Co(III)]^+$.

The spectral changes which result during the second oxidation of **2** are shown in Figure 2c and are consistent with the abstraction of an electron from the corrole part of the molecule in the second step. The spectral pattern of doubly oxidized **2** (Figure 2c) is similar to that of the singly oxidized dyad giving further evidence that the porphyrin part of the molecule is only slightly affected by the extraction of a second electron at a controlled potential of 0.80 V.

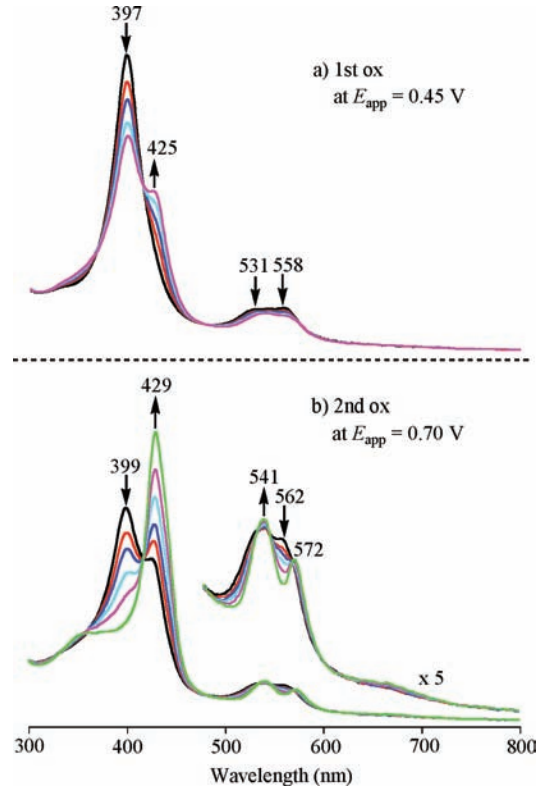

Figure 3. UV−visible spectral changes of $(PCOx)Co_2$ **5** during the (a) first and (b) second oxidations in PhCN containing 0.1 M TBAP.

In summary, the UV−visible spectral changes during the first and second oxidations of dyad **2** (Figure 2) are self-consistent and indicate that the first electron abstraction occurs on the porphyrin part of the molecule (at $E_{1/2}$ = 0.38 V) followed by a second electron abstraction from the corrole part of the dyad at $E_{1/2}$ = 0.53 V. It should also be noted that the latter half-wave potential is quite close to the $E_{1/2}$ = 0.57 V for the metal-centered oxidation of the monocorrole **8** (Figure 1), further suggesting a corrole-centered oxidation in the second process. Similar assignments for the site of electrooxidations can be made for dyads **1** and **3** where the porphyrin is oxidized first followed by an electron abstraction from the corrole to give the doubly oxidized species.

In contrast to what occurs for **1**−**3**, the spectroelectrochemical data of **4**-**6** implies a different electrooxidation mechanism under the same solution conditions. An example of the spectral changes is shown in Figure 3 for the case $(PCOx)Co_2$ **5** which is oxidized at $E_{1/2}$ = 0.45 and 0.52 V in PhCN (Figure 1d). A comparison of the spectral changes in Figure 3 with that in Figure 2 and with the corresponding monocorrole $(F_5PhMes_2Cor)Co$ **8** (see spectra in ref 26) indicates clearly that the first electron abstraction of dyad **5** occurs at the corrole part of the molecule and the second at the porphyrin where major spectral changes are observed and the final oxidation product has a well-defined Soret band at 429 nm and two Q bands at 541 and 572 nm, both consistent with a Co^{III} porphyrin. The $E_{1/2}$ = 0.45 V for the first oxidation of **5** can also be compared to an $E_{1/2}$ = 0.47

Scheme 2. First Two Oxidations of Dyads **1**−**6**[a]

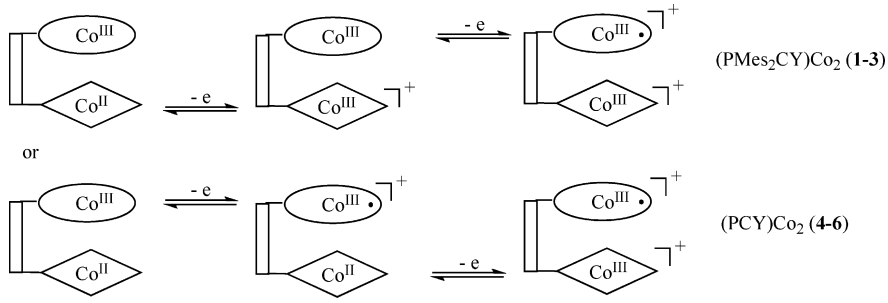

[a] Same macrocycle notation as in Scheme 1.

V for the first oxidation of the monocorrole (Me_4Ph_5Cor)Co **9** (Figure 1), and this gives further evidence that the corrole is the site of the first electron abstraction.

Similar spectral changes are seen for the dyads **4** and **6** where the corrole is oxidized prior to the porphyrin in PhCN containing 0.1 M TBAP under an N_2 atmosphere. In summary, the results of thin-layer spectroelectrochemistry indicates that the porphyrin unit is oxidized prior to the corrole unit in the dyads **1**−**3** but the opposite occurs for the dyads **4**−**6** where the first oxidation of the neutral compound involves the corrole and not the porphyrin under the electrochemical conditions of Figure 1. These different pathways are shown in Scheme 2 and have a direct relevance to the number of electrons transferred in the catalytic reduction of O_2 in acid media as described in later sections of the manuscript.

Carbon Monoxide Binding Effect on Electrochemistry of (F_5PhMes_2Cor)Co (8), (Me_6Et_2PhPor)Co (7), and ($PMes_2COx$)Co_2 (2). It has long been known that carbon monoxide will axially bind to Co(III) corroles[37,53] and Co(III) porphyrins[42,43,54] but not to the higher or lower metal oxidation states of these two macrocycles. Because the dyads **1**−**6** contain a Co^{II} porphyrin and a Co^{III} corrole, an initial oxidation at the porphyrin unit would be accompanied by a binding CO under a CO atmosphere and a negative potential shift in $E_{1/2}$ as compared to the same reaction under N_2 while an oxidation at the corrole part of the molecule would be accompanied by a loss of CO and a positive shift in $E_{1/2}$ under the same solution conditions. This being the case, the initial site of electron transfer in the dyad can be assigned quite definitively by monitoring how $E_{1/2}$ shifts upon going from N_2 to CO above the solution.

The above-described shifts of $E_{1/2}$ upon going from N_2 to CO as the gas above the solution are clearly seen in the electrochemical behavior of the monomeric macrocycles **8** and **7** in Figure 4. The first oxidation of the monocorrole **8** shifts from 0.73 V under N_2 to 0.86 V under CO (Figure 4a) and there is no change in $E_{1/2}$ for the following two reactions as expected since CO does not bind to the higher oxidized form of the macrocycle. This contrasts with the case

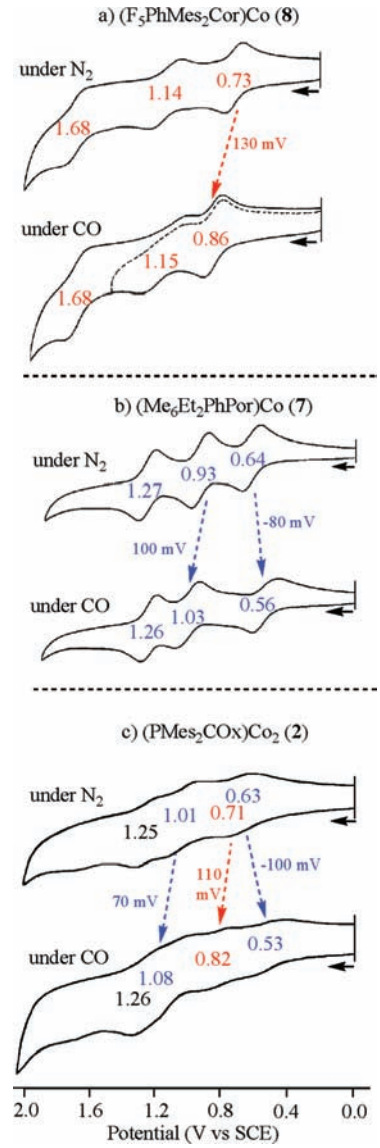

Figure 4. CVs of **8** (a), **7** (b), and **2** (c) in CH_2Cl_2 containing 0.1 M $TBAPF_6$ under N_2 and CO atmosphere.

of the monoporphyrin **7** where the first oxidation shifts negatively (from 0.64 to 0.56 V) and the second positively (from 0.93 to 1.03 V) as CO is added to the electrogenerated Co^{III} porphyrin and then lost upon further oxidation. The third oxidation of **7** is virtually unchanged in the $E_{1/2}$ value as should be the case.

(53) Paolesse, R. In *The Porphyrin Handbook*; Kadish, K. M., Smith, K. M., Guilard, R., Eds.; Academic Press: San Diego, CA, 2000; Vol. 2, pp 201−232.
(54) Schmidt, E.; Zhang, H.; Chang, C. K.; Babcock, G. T.; Oertling, W. A. *J. Am. Chem. Soc.* **1996**, *118*, 2954–2961.

Table 2. Electroreduction of Dioxygen by Adsorbed Biscobalt Porphyrin-Corrole Dyads

	$(PMes_2CY)Co_2$ (**1**−**3**)			$(PCY)Co_2$ (**4**−**6**)		
bridge (Y)	E_p[a]	$E_{1/2}$[b]	n[c]	E_p[a]	$E_{1/2}$[b]	n[c]
O	0.25	0.32	2.4	0.34	0.41	3.5[25]
Ox	0.27	0.33	2.5	0.35	0.40	3.1
X	0.25	0.32	2.5	0.38	0.45	3.7[25]

[a] Peak potential of the dioxygen reduction wave (V vs SCE). [b] Half-wave potential (V vs SCE) for dioxygen reduction at rotating disk electrode (ω = 100 rpm). [c] Electrons consumed in the reduction of O_2 as estimated from the slope of the Koutecky−Levich plots.

A similar shift of $E_{1/2}$ is expected to occur in the dyads containing one porphyrin and one corrole, and this is clearly seen by the CVs for **2** in Figure 4c. Upon changing from N_2 to CO, the first oxidation shifts negatively from 0.63 to 0.53 V indicating a porphyrin-centered oxidation while the second shifts positively from 0.71 to 0.82 V, consistent with oxidation at the corrole unit of the dyad. The third oxidation of **2** also shifts positively from 1.01 to 1.08 V under CO. This is similar to what is seen for the monoporphyrin (Figure 4b) and as expected for oxidation of a Co^{III} porphyrin which is accompanied by loss of the bound CO. These reactions are consistent with the above results from spectroelectrochemistry of compound **2**.

Catalysis of O_2 Reduction by Dyads. The electrocatalytic properties of the biscobalt porphyrin-corrole dyads **1**−**3** were examined in 1 M $HClO_4$. The catalytic activity of the biscobalt complexes toward the reduction of O_2 was determined by cyclic voltammetry, as well as by rotating disk electrode voltammetry, and the results are summarized in Table 2. In an air saturated solution, the CVs at a $(PMes_2CY)Co_2$-coated electrodes are characterized by a large reduction peak at E_{pc} = 0.25 to 0.27 V, the exact potential depending upon the spacer of the dyad (see measured potentials in Table 2). All three compounds catalyze the electroreduction of O_2 at potentials close to $E_{1/2}$ values observed for (TPFCor)Co and $(F_5PhMes_2Cor)Co$ as seen in our previously studies (E_{pc} = 0.24 − 0.25 V).[26] The average $E_{1/2}$ value for the electroreduction of O_2 at a rotating disk electrode coated with the three $(PMes_2CY)Co_2$ dyads (**1**−**3**) is 0.32 V while (TPFCor)Co and $(F_5PhMes_2Cor)Co$ show a similar average $E_{1/2}$ value of 0.30 V.[26]

The number of electrons transferred in the O_2 electroreduction process involving complexes **1**−**3** ranges from 2.4 to 2.5 as determined by rotating disk voltammetry (Table 2 and Figure 5). This indicates that the electrocatalytic reduction of O_2 by the biscobalt porphyrin-corrole dyads leads to formation of H_2O_2 through a process involving a $2e^-$ reaction. This catalytic behavior is similar to what was earlier reported for $(PCY)H_2Co$[25] and $(PCY)MClCoCl$[23] where the catalytic reduction of O_2 occurred at an average half-wave potential of 0.34 V. The average n value for the heterobimetallic compounds was 2.7 electrons[23] transferred in the reduction of O_2 as compared to an average n = 2.5 for the three currently examined $(PMes_2CY)Co_2$ dyads under the same experimental conditions. These values are clearly different from the biscobalt porphyrin-corrole dyads **4**−**6** where n = 3.1 to 3.7 (Table 2), and O_2 was mainly reduced to H_2O through a four-electron, four-proton process. Even after replacing the rigid PCO (**4**) spacer by PCOx (**5**) which is more flexible, the number of electrons transferred remains higher (n = 3.1) than that observed for $(PMes_2COx)Co_2$ **2** (n = 2.5). One possible explanation for the low catalytic efficiency of the mesityl-containing porphyrin-corrole dyads $(PMes_2CY)Co_2$ in the direct reduction of O_2 to H_2O is that steric interactions must occur between the bulky substituents of the corrole and the porphyrin macrocycle and thus induce ring lateral slippage[46] which could disfavor the accommodation of oxygen intermediates during multielectron catalysis. The presence of electron-withdrawing *meso*-substituents in $(PMes_2CY)Co_2$ compared to $(PCY)Co_2$ may also disfavor cleavage of the two formal O−O bonds required for the direct reduction of O_2 to H_2O. This substituent effect was proposed by Chang et al.[15] to explain the low catalytic efficiency toward O_2 by cofacial Pacman porphyrins bearing an aryl group *trans* to the spacer. The authors also reported that the presence of aryl *meso*-substituents in cofacial diporphyrins will lower the potential of O_2 reduction by an average of 130 mV compared to the unsubstituted derivatives, and this is in accord with the decrease in potential observed between $(PCY)Co_2$ (**4**-**6**) ($E_{1/2}$ = 0.43 V) and $(PMes_2CY)Co_2$ (**1**−**3**) ($E_{1/2}$ = 0.32 V) in the current study (Table 2).

Electron Spin Resonance (ESR) Characterization of the Doubly Oxidized Dyads 1−3. The oxidation of **1**−**3** with O_2 in the presence of $HClO_4$ in PhCN gives the ESR spectra illustrated in Figure 6. The observed g-values of 2.0046 are characteristic of an organic radical and quite different from the large g-value (2.037) observed for Co(IV) porphyrin complexes[55] and consistent with our earlier assignment of the oxidation state of the singly oxidized monocorrole.[26] Thus, the doubly oxidized species **1**−**3** in PhCN containing $HClO_4$ is in all three cases assigned as $(Por)Co(III)^+$-$(Cor^{\bullet})^+Co(III)$.

Catalytic Reduction of O_2 in the Homogeneous Phase. The catalytic reduction of O_2 with the biscobalt porphyrin-corrole dyads **1**−**6** was confirmed for the homogeneous phase using 1,1′-dimethylferrocene $Fe(C_5H_4Me)_2$ as a reductant in PhCN. No oxidation of $Fe(C_5H_4Me)_2$ by O_2 occurred in the presence of $HClO_4$ in PhCN at 298 K. However, the addition of **1**−**6** to an air-saturated PhCN solutions of $Fe(C_5H_4Me)_2$ and $HClO_4$ resulted in efficient oxidation of $Fe(C_5H_4Me)_2$ by O_2. When **1**, **2**, **4**, or **5** is used as a catalyst, the concentration of $[Fe(C_5H_4Me)_2]^+$ formed in the catalytic reduction of O_2 by $Fe(C_5H_4Me)_2$ is two times the O_2 concentration (1.7×10^{-3} M) as shown in Figure 7. Thus, the two-electron reduction of O_2 by $Fe(C_5H_4Me)_2$ occurs efficiently in the presence of a catalytic amount of **1**, **2**, **4**, or **5** and excess $HClO_4$ (2.0×10^{-2} M) in PhCN. There was no further reduction to produce more than 2 equiv of $[Fe(C_5H_4Me)_2]^+$. In contrast to this, the amount of $[Fe(C_5H_4Me)_2]^+$ formed is doubled when **3** or **6** was used as a catalyst as compared with the case of **1** or **2**, as shown by the blue lines in Figure 7. Thus, the four-electron reduction of O_2 occurs efficiently in the presence of a catalytic amount of **3** or **6** and excess $HClO_4$ (2.0×10^{-2} M) in PhCN (eq 1).

(55) Fukuzumi, S.; Miyamoto, K.; Suenobu, T.; Van Caemelbecke, E.; Kadish, K. M. *J. Am. Chem. Soc.* **1998**, *120*, 2880–2889.

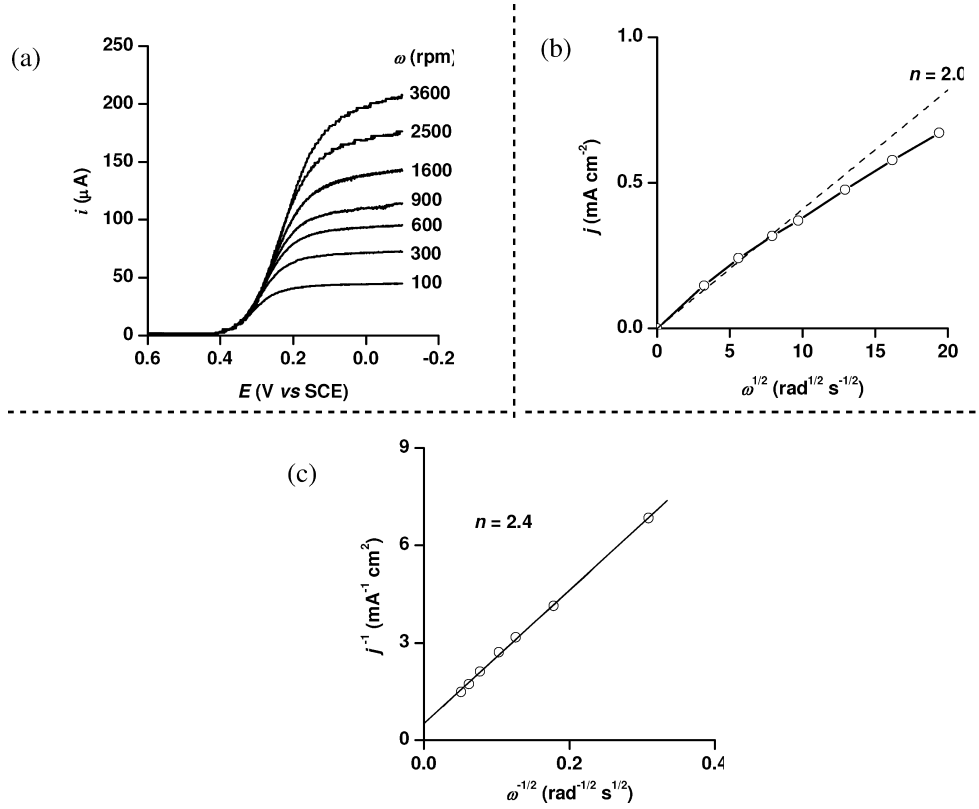

Figure 5. Catalyzed reduction of O_2 in 1 M $HClO_4$ at a rotating graphite disk electrode coated with $(PMes_2CO)Co_2$ **1**. (a) Values of the rotation rates of the electrode (ω) are indicated on each curve. The disk potential was scanned at 5 mV s^{-1}. (b) Levich plots of the plateau currents of (a) vs (rotation rate)$^{1/2}$. The dashed line refers to the theoretical curve expected for the diffusion-convection limited reduction of O_2 by $2e^-$. (c) Koutecky−Levich plots of the reciprocal plateau currents vs (rotation rates)$^{-1/2}$. Supporting electrolyte: 1 M $HClO_4$ saturated with air.

$$4Fe(C_5H_4Me)_2 + O_2 + 4H^+ \xrightarrow[(PMes_2CX)Co_2\ (\mathbf{3})]{} 4[Fe(C_5H_4Me)_2]^+ + 2H_2O \quad (1)$$

The same selectivity with regard to the two-electron versus four-electron reduction of O_2 by 1,1′-dimethylferrocene depending on the type of linkage (Y) of biscobalt complexes was observed for the catalytic reduction of O_2 with cofacial biscobalt porphyrins in the presence of $HClO_4$ in PhCN.[20,21] The suitable metal−metal separation with Y = 9,9-dimethylxanthene (X) is required to produce the μ-peroxo Co(III)-O_2^{2-}-Co(III) complex that is the key intermediate for the catalytic four-electron reduction of O_2.[20,21] The number of electrons transferred in the O_2 electroreduction at the electrode process involving complexes **1**−**6**(Table 2 and Figure 5) is different from that observed in the homogeneous phase except for **6** (n = 3.7). The different number of electrons transferred in the O_2 electroreduction process at the electrode in Table 2 may result from the different geometry of biscobalt complexes adsorbed on the graphite electrode.

The catalytic mechanism of the two-electron versus four-electron reduction of O_2 with biscobalt complexes is summarized in Scheme 3. Judging from the observed ESR spectra in Figure 6, the biscobalt complex (Por)Co(II)-(Cor)Co(III) is oxidized by O_2 in the presence of $HClO_4$ to produce the two-electron oxidized species (Por)Co(III)-(Cor$^{\bullet}$)$^+$Co(III). Electron transfer from Me_2Fc to both (Por)Co(III) and (Cor$^{\bullet}$)$^+$Co(III) moieties of (Por)Co(III)-(Cor$^{\bullet}$)$^+$Co(III) is thermodynamically feasible based on the redox potentials

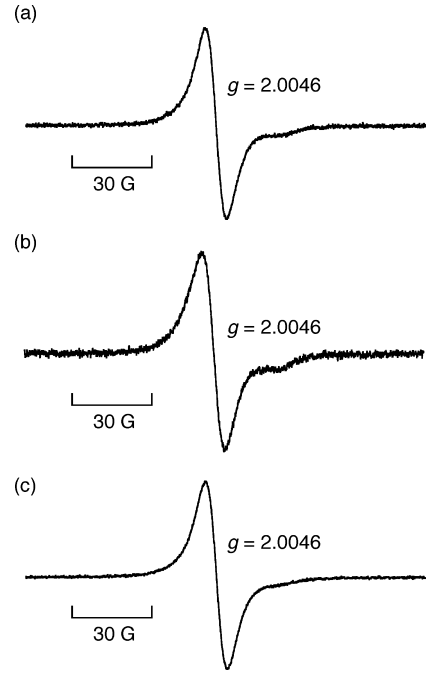

Figure 6. ESR spectra of doubly oxidized **1**−**3** produced by the chemical oxidation of (a) **1**, (b) **2**, and (c) **3** (3.0×10^{-4} M) with O_2 and $HClO_4$ (2.0×10^{-2} M) in PhCN at 298 K.

in Table 1, when 2 equiv Me_2Fc is oxidized to Me_2Fc^+ accompanied by regeneration of (Por)Co(II)-(Cor)Co(III). This is the catalytic two-electron reduction of O_2 (the upper catalytic cycle in Scheme 3). The reactive intermediate for the two-electron reduction of O_2 may be the peroxo species

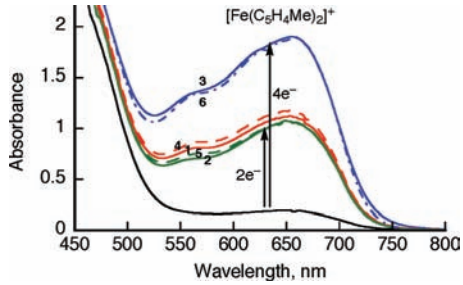

Figure 7. Visible absorption spectra changes in the catalytic reduction of O_2 (1.7×10^{-3} M) by $Fe(C_5H_4Me)_2$ (2.0×10^{-2} M) in the presence of $HClO_4$ (2.0×10^{-2} M) and **1**−**6** (2.0×10^{-5} M) in PhCN at 298 K; **1** (red solid line), **2** (green solid line), **3** (blue solid line), **4** (red broken line), **5** (green broken line), and **6** (blue broken line). Black: in the absence of cobalt complex.

Scheme 3

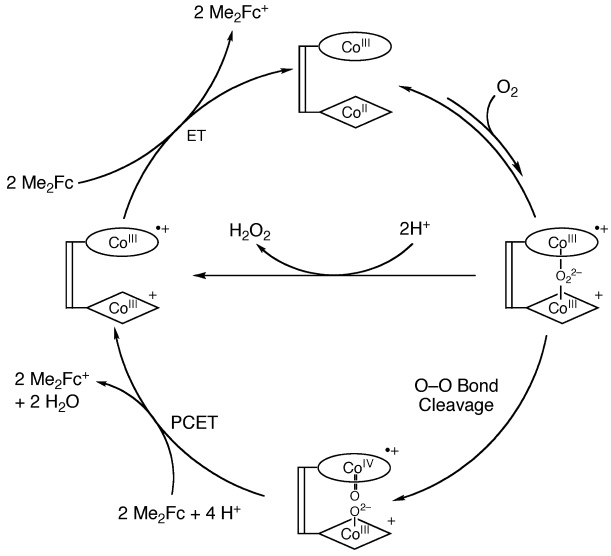

(Por)Co(III)-(O_2^{2-})-(Cor$^{\bullet}$)$^+$Co(III), which undergoes competition between the protonation of the peroxo moiety and the O−O bond cleavage as shown in Scheme 3. The protonation leads to the two-electron reduction of O_2 to produce H_2O_2, whereas the O−O bond cleavage leads to the four-electron reduction of O_2 via formation of (Cor$^{\bullet}$)$^+$Co(III)-oxo species that is reduced by 2 equiv of Me_2Fc to produce H_2O and (Cor)Co(III). The stronger binding of the two Co(III) centers with the peroxo moiety along with the suitable metal−metal separation in the case of Y = 9,9-dimethylxanthene (X) may facilitate the O−O bond cleavage, leading to the four-electron reduction of O_2.

Conclusions

The results of the present study have demonstrated that the catalytic behavior of biscobalt porphyrin-corrole dyads toward the catalytic electroreduction of dioxygen is strongly influenced by both the position of substituents on the corrole ring and the type of linkage (Y) which determines the distance between the two cobalt macrocycles. As mentioned earlier in the manuscript, our intended goal in preparing the *meso*-substituted corroles in dyads **1**−**3** was to increase the Lewis acid character of the macrocycle to shift the formal Co^{III}/Co^{IV} process to a more positive potential and thus enhance the $4e^-$ reduction of dioxygen to water. Although the desired positive shift in $E_{1/2}$ was observed for the monomeric corroles in nonaqueous media under N_2,[26] an unexpected opposite effect is observed in the electrocatalytic activity where the newly investigated dyads with mesityl substituents on the corrole show a preference for H_2O_2 rather than H_2O formation in acid media while also undergoing a negative rather than positive shift in $E_{1/2}$ for the electrocatalytic process.

The position of corrole substituents (β-pyrrole versus *meso*-carbon) are less important in the homogeneous catalytic reduction of O_2 and here the type of bridge (and the spacing between the two macrocycles) becomes the dominant factor. A quantitative four-electron reduction of O_2 by 1,1′-dimethylferrocene occurs only with the biscobalt complexes **3** and **6** which have a suitable metal−metal separation given by the spacer Y = 9,9-dimethylxanthene (X), to produce the μ-peroxo Co(III)-O_2^{2-}-Co(III) complex and O−O bond cleavage, which is in competition with the protonation. The same spacer was found to be optimum in the case of biscobalt and bisporphyrins.[22b]However, the fact that the catalytic behavior of dyad **3** in solution differs from the electrocatalytic mechanism emphasizes the importance of selecting not only the "correct" spacer but also the "correct" corrole macrocycle substituents to obtain a four-electron reduction both in solution and at an electrode surface. The data in the current study also indicates that face-to-face dyads containing a Co(II) porphyrin and a Co(III) corrole or a Co(II) porphyrin and a singly oxidized Co(III) corrole are both effective catalysts for the four-electron reduction of dioxygen to water, again assuming that both forms of the compounds have the "correct" spacer, for example, in this work 9,9-dimethylxanthene (X). On the basis of these results, the next step in obtaining an optimum catalyst for O_2 reduction would be to modify both the porphyrin and corrole substituents to obtain the most positive redox potentials. This has yet to be attempted.

Acknowledgment. The support of the Robert A. Welch Foundation (K.M.K., Grant E-680), the French Ministry of Research (MENRT), CNRS (UMR 5260) and a Global COE program, "the Global Education and Research Center for Bio-Environmental Chemistry" from the Ministry of Education, Culture, Sports, Science and Technology, Japan are gratefully acknowledged.

IC802092N